Journal of Thermal Analysis and Calorimetry (2021) 143:3331–3343
https://doi.org/10.1007/s10973-020-09300-y

An efficient enhancement in thermal conductivity of water-based hybrid nanofluid containing MWCNTs-COOH and Ag nanoparticles: experimental study

Rashid Pourrajab[1] · Aminreza Noghrehabadi[1] · Mohammad Behbahani[2] · Ebrahim Hajidavalloo[1]

Received: 13 September 2019 / Accepted: 7 January 2020 / Published online: 16 January 2020

Abstract
Synergistic effect of MWCNTs-COOH and Ag nanoparticle on improving thermal conductivity of hybrid nanofluid has been explained experimentally in this paper. Different concentrations of MWCNTs/water nanofluids (0.004, 0.008, 0.04 and 0.16 vol%) were used and mixed with (0.04 vol%) Ag nanoparticle to prepare hybrid nanofluid. TEM was employed for confirming the size of MWCNTs and Ag nanoparticles in base fluids. Furthermore, SEM and XPS were utilized to characterize the prepared hybrid nanofluid. The hybrid nanofluids' thermal conductivity was measured in varying volume fractions at 20–50 °C temperatures. As shown by the results, the ratio of thermal conductivity of hybrid nanofluids is increased in a nonlinear manner as the concentration and temperature increase. It was seen that the hybrid nanofluid's thermal conductivity having 0.04 vol% Ag nanoparticles and 0.16 vol% MWCNTs was synergistically improved by 47.3% in comparison with thermal conductivity the water base fluid. In the end, new thermal conductivity ratio correlation was suggested on the basis of the empirical data. Comparisons of correlation output and experimental thermal conductivity ratio data showed high accuracy and capability in modeling of thermal conductivity ratio data.

Keywords Hybrid nanofluid · Thermal conductivity · MWCNTs-COOH · Ag · New correlation

List of symbols

Ag	Silver
K	Thermal conductivity (W m^{-1} K^{-1})
MWCNT	Multi-wall carbon nanotubes
SEM	Scanning electron microscope
T	Temperature (°C)
TEM	Transmission electron microscopy
THW	Transient hot wire
DI	Deionized
u	Uncertainty (%)
vol	Volume fraction
XRD	X-ray crystallography
XPS	X-ray photoelectron spectroscopies
w	Mass of nanoparticles (g)

Greek

φ	Nanoparticle concentration

Subscripts

bf	Base fluid
Corr	Correlation
Exp	Experimental
NP	Nanoparticles
nf	Nanofluid
hnf	Hybrid nanofluid

Introduction

Coolant fluids have many applications in the modern equipment and industries. The heat carrier is commonly used as the heat transfer medium in industrial production that causes heat transfer in a uniform manner. Among a large number of heat carriers, water is mostly employed in the heat recovery system [1] and solar collector field [2]. Despite various advantages of water like low viscosity and high heat transfer efficiency, it has a great the biggest flaw, which is its slow heating and thermal inertia; thus, it is not able to satisfy the requirement of modern industry. When the water thermal

✉ Mohammad Behbahani
mohammadbehbahani89@yahoo.com

[1] Department of Mechanical Engineering, Shahid Chamran University of Ahvaz, Ahvaz, Iran

[2] Faculty of Engineering, Shohadaye Hoveizeh University of Technology, Dashte Azadegan, Iran

conductivity is improved, the heating speed will rise. In addition, the cooling time is decreased, reducing the volume of heat transfer device and amount used working fluid. Up to now, the work "nanofluid" was originally invented by Choi [3] in 1995 in Argonne National Laboratory, USA, as a novel kind of fluid by swinging copper nanoparticles in water to improve their thermo-physical property. After that, various types of nanofluids were developed by different researchers, and heat transfer behavior of these nanofluids was determined aiming at using the nanofluids as a new generation of fluids, which show auspicious potential considering cooling and heat transfer [4–9]. Generally, nanoparticles are aluminum oxide (Al_2O_3) [10, 11], iron (III) oxide (Fe_3O_4) [12, 13] and copper oxide (CuO) [14, 15]. Out of all the physical characteristics of the nanofluids, thermal conductivity is considered as the main thermo-physical characteristics, with a significant impact on developing very effective heat transfer devices like industrial heat exchangers [16], automobile radiators [17], solar heat exchanger [18], energy systems, solar collectors [19, 20] and solar power plants [21]. Zeng and Xuan [22] investigated the high light absorption efficiency and enhanced heat transfer performance of nanofluids being composed of SiO_2/Ag plasmonic nanoparticles and multi-wall carbon nanotubes (MWCNTs) used for volumetric solar collectors. In this scenario, the functional fluids called nanofluids are a group of heat transfer fluids that contain thermally conductive nanometer-sized particles (range 100 nm). These particles are spread in the fluid medium. Adding very small amounts of nanoparticles in water, oils and other liquids improves optical, magnetic and electronic properties [23]. Unique characteristics are observed for carbon nanotubes among one-dimensional nanostructures. Some of these notable properties include chemical stability, physical strength, high thermal and electrical conductivity, and mechanical resistance. Since early 1990s, many researchers have been attracted by carbon nanotubes through these properties. Since the discovery of carbonaceous materials with high thermal conductivity like graphene, carbon nanotubes (CNT) and graphene oxide (GO), many research works have been allocated to carbonaceous materials-based nanofluids [24–27]. A new class of hybrid nanomaterials was developed by development of carbon nanotubes, which include a combination of carbon nanotubes with metallic, semi-conductive or non-conductive nanoparticles. Single material lacks all demanded properties and characteristics. Hence, trade-off between rheological and thermal characteristics is required. In this case, using hybrid nanofluids is easy since they show improved thermal conductivity due to synergetic impact [28–31]. Carbon nanotubes (CNTs) and multi-walled carbon nanotubes (MWCNTs) are among the widely used nanoparticles [32–35]. In addition, they are used for constructing hybrid nanofluids. As the advantages of hybrid nanofluids have been recognized, thermal researchers and scientists have started investigating thermal conductivity properties and synthesis of these materials. Turcu et al. [36] originally prepared a hybrid nanostructure by adding Fe_3O_4 nanoparticles on MWCNTs using polypyrrole polymerization. Jha and Ramaprabhu [37] diffused Au-MWNTs, Pd-MWNTs and Ag-MWNTs in de-ionized water and ethylene glycol. Ag-MWNTs showed a better enhancement of thermal conductivity, i.e., 11.30% and 37% and with de-ionized water and ethylene glycol, at a volume fraction of 0.03% as given by Rostamian et al. [38]; the nanofluid thermal conductivity was enhanced up to 36% using 0.75 vol% CuO-SWCNTs hybrid material. According to Megatif et al. [39], thermal conductivity of CNT nanofluids was more than CNT/TiO_2 hybrid nanofluid. Nine et al. [40] investigated impacts of nanoparticle shape, non-grounded and grounded MWCNTs on (Al_2O_3-MWCNTs/water) hybrid nanofluid's thermal conductivity. Raising ratio of MWCNTs increased thermal conductivity in hybrid nanofluid. The nanoparticles with cylindrical shape had higher enhancement in thermal conductivity in comparison with the particles with spherical shape. It was observed that non-grounded MWCNTs gained higher improvement in thermal conductivity compared to grounded MWCNTs. Shahsavar et al. [41] indicated an impact of sonication on thermal conductivity of (CNTs + Fe_3O_4/DI water) hybrid nanofluid. The maximum concentration of CNTs (1.535%) + Fe_3O_4 (2.428%) with sonication time of 5 min and 25–55 °C temperature range provided the maximum improvement in thermal conductivity of 26.07–34.26%. Chen et al. [42] evaluated effective thermal conductivity of Fe_2O_3-MWNT hybrid nanofluid and indicated that the hybrid fillers have a synergistic impact on heat conductive networks. They showed 28% improvement for hybrid nanofluid's thermal conductivity that is higher than thermal conductivity of mono nanofluids. Zadkhast et al. yielded the thermal conductivity of hybrid nanofluids, composed by MWCNT-CuO nanoparticles, and dispersed in the water base fluid at different nanoparticle concentration and temperature. According to their results, the maximum thermal conductivity was increased by 30.38% at 50 °C and $\varphi = 0.6\%$ [43]. Farbod and Ahangarpour [44] studied the thermal conductivity properties nanofluids with the water base, which contained Ag-decorated MWCNTs. They developed some samples with functionalized and pristine MWCNTs and varying mass ratios of Ag/MWCNT, reflux times, different Ag/MWCNTs concentrations and Ag- undecorated and decorated MWCNTs. A considerable enhancement was seen in the thermal conductivity in the MWCNT nanofluids having Ag-decorated MWCNTs in comparison with thermal conductivity of the undecorated samples. Munkhbayar et al. [45] reported effect of silver nanoparticle loadings (1 mass%, 2 mass%, and 3 mass%) on MWCNTs/water nanofluid's thermal conductivity. The results of measurement indicated that a fluid having 0.05 mass% MWCNTs–3 mass% Ag

composite presented the maximum enhancement of thermal conductivity (14.5% at 40 °C). However, there are a number of studies concerning the nanofluids with Ag nanoparticles added to CNTs. Also, the obtained results still not satisfy as expected. One of the common procedures in the last decade was modeling by curve fitting of thermal conductivity data. Thus, new correlations for thermal conductivity prediction need to be developed. In this context, for the first time we present the results of the effects of MWCNTs-COOH loadings (0.004 vol%, 0.008 vol%, 0.04 vol% and 0.16 vol%) on thermal conductivity of Ag/water-based nanofluid and developed correlations for predicting thermal conductivity of MWCNTs-COOH/Ag/water hybrid nanofluid.

Experimental

Hybrid nanofluid preparation

MWCNTs-COOH and silver nanoparticles have been used for the preparation of hybrid nanofluid as the following reasons:

(a) Dispersity and stability of MWCNTs-COOH decorated with silver nanoparticles are higher than unmodified MWCNTs, and the mentioned phenomenon is very important for increasing the thermal conductivity and application as heat transfer nanofluid.
(b) The thermal conductivity of MWCNTs-COOH decorated with silver nanoparticles is higher than MWCNTs-COOH, and the obtained data from experiment can prove the mentioned claim. The possible reason is that silver itself is a good thermal conductor (k Ag = 419 W m^{-1} K^{-1}), the boundary scattering losses [46], and interfacial resistance to heat flow [47] between Ag/MWCNTs-COOH and base fluid can be reduced. Therefore, the decoration of MWCNTs-COOH with AgNPs offers an excellent means to recover the potential reduction in thermal conductivity arising from functionalization of MWCNTs.

The MWCNTs-COOH and Ag nanoparticles were prepared by the US Research Nanomaterials, Inc. Table 1 gives the specifications and detailed information about the nanomaterials. Diffusing CNTs in a base fluid is one of the main steps when the carbon nanofluids are prepared. Because of strong van der Waals forces between carbon surfaces as well as the high aspect ratio, the CNTs dispersion in aqueous media is a challenging task. CNTs have a hydrophobic nature. Therefore, it is not possible to disperse them in water under normal conditions [48, 49]. In two ways, it is possible to have stable nanofluids with carbon nanotubes. The first way is using a surfactant like Arabic gum. In the second way, the carbon nanotubes can be functionalized. Undesired impacts may be observed on the thermal conductivity of the suspensions by adding a surfactant. Thus, it seems that use of functionalized carbon nanotubes is more suitable. Functionalizing MWCNTs by the use of COOH functional groups provide hydrophilic carbon nanotubes. Therefore, the stability of the prepared nanofluids is enhanced [50].

In the current study, a two-step approach, which is extensively used by the researchers [6, 51–54], is utilized for preparation of the MWCNTs-COOH/Ag/water hybrid nanofluid in varying concentrations using water as the base fluid. In this approach, the nanoparticles, which are individually developed, are diffused in the base fluid using appropriate dispersion methods. In the first step, a DI-water-based Ag nanofluid with a nanoparticle concentration of 0.04 vol% was made by a two-step approach because of its low cost and simplicity compared to the one-step approach. Finally, the MWCNTs-COOH/Ag/water hybrid nanofluids were developed with a fixed concentration of Ag (0.04 vol%) and MWCNT with four varying concentrations (0.004 vol%, 0.008 vol%, 0.04 vol% and 0.16 vol%). The distribution and size of nanoparticle in the base fluid have an important role in specifying the hybrid nanofluid's cooling and thermal behavior. Thus, the main problem with the two-step approach is preventing from adherence and agglomeration of nanoparticles. For this purpose, the hybrid nanofluid was mixed for 15 min by the use of Homogenizer (MICCRA D-9) and a mechanical stirrer (IKA RW20). Afterward, ultrasonic waves were presented to the nanofluid for 5 min using a power of 400 W and a frequency of 24 kHz by Ultrasonic Homogenizer (UP400S, Hielscher GmbH) in order to dismantle agglomerated particles, allowing these particles to be resolved in the hybrid nanofluid. Ice water was added to the ultrasonic bath repeatedly during ultrasonication so that the suspension temperature is not increased. A schematic preparation of water-based MWCNTs-COOH/Ag hybrid nanofluid and thermal network of nanomaterials is shown in

Table 1 Basic information of nanoparticles

Material	Average diameter/nm	Surface area/ m^2 g^{-1}	Density/g cm^{-3}	Thermal conductivity/w m^{-1} k^{-1}
Ag nanoparticle	5–8	25–42	10.9	Approximately 419
CNTs	20–30 (OD)	110	2.6	Approximately 3000

Fig. 1. The stabilities of the hybrid nanofluids were studied (with the naked eye) approximately 3 days after ultrasonication, and no sedimentation was observed in the samples.

Experimental sets and thermal conductivity measurement

A KD2 Pro (Decagon Devices, Inc., USA) thermal properties analyzer with a maximum error of almost 5% was employed in the current work so that the thermal conductivity of functionalized MWCNTs/Ag–water nanofluids is measured. More detailed information about KD2 Pro thermal analyzer device is listed in Table 2. This analyzer provides measurement of the fluids' thermal conductivity on the basis of the transient hot wire approach [55, 56] using a KS-1 (stainless steel single needle) sensor. Having a diameter of 1.27 mm and a length of 60 mm, this sensor is inserted vertically into the hybrid nanofluid located in a stable temperature bath (WNE 7, Memmert GmbH+ Co.KG, Germany) with 2 Pt100 sensors Class A used to keep a constant temperature during the test with an accuracy of 0.1 °C. The transient hot wire approach is a reliable and quick method where a heat pulse is applied to a needle. In this method, the temperature response with time is monitored during and after the heat pulse at besides needle both. The temperature response nature is a follow-up of the thermal characteristics of the material. Prior to measuring the nanofluids' thermal conductivity, DI water as base fluid was used for calibration of the device. The measurements of the thermal conductivity were reiterated for three times. The samples' thermal conductivity was measured in the temperature range of 20–50 °C. For having an acceptable accuracy in the experiments, the needle

Table 2 Specifications of KD2 Pro thermal analyzer device measurement (certificate of quality assurance)

Measurement speed	Accuracy	Operating environment	Sensor	Serial number
1 min	±5% thermal conductivity	0–50°C	KS-1-00086	KP2620

of the device should be totally immersed in the fluid, and its orientation in the sample vials should be vertical. In addition, measurement of thermal conductivity should be carried out in a completely relaxed condition with no vibration and movement in fluid environment. In order to ensure results of measurement, each sample was tested repeatedly several times at different temperatures, and the average values were regarded as the empirical data. It was seen that the thermal conductivity of the base fluid, which was measured experimentally, showed a highly low difference with pure water in ASHRAE Handbook [57] and in good agreement. Figure 2 indicates the results. According to the experimental data, the thermal conductivity enhancement and the thermal conductivity ratio are expressed as follows:

$$\text{Thermal conductivity ratio} = \frac{k_{\text{hnf}}}{k_{\text{bf}}} \tag{1}$$

$$\text{Thermal conductivity enhancement}\,(\%) = \frac{k_{\text{hnf}} - k_{\text{bf}}}{k_{\text{bf}}} \times 100 \tag{2}$$

where k_{hnf} and k_{bf} denote the thermal conductivity of hybrid nanofluid and thermal conductivity of base fluid.

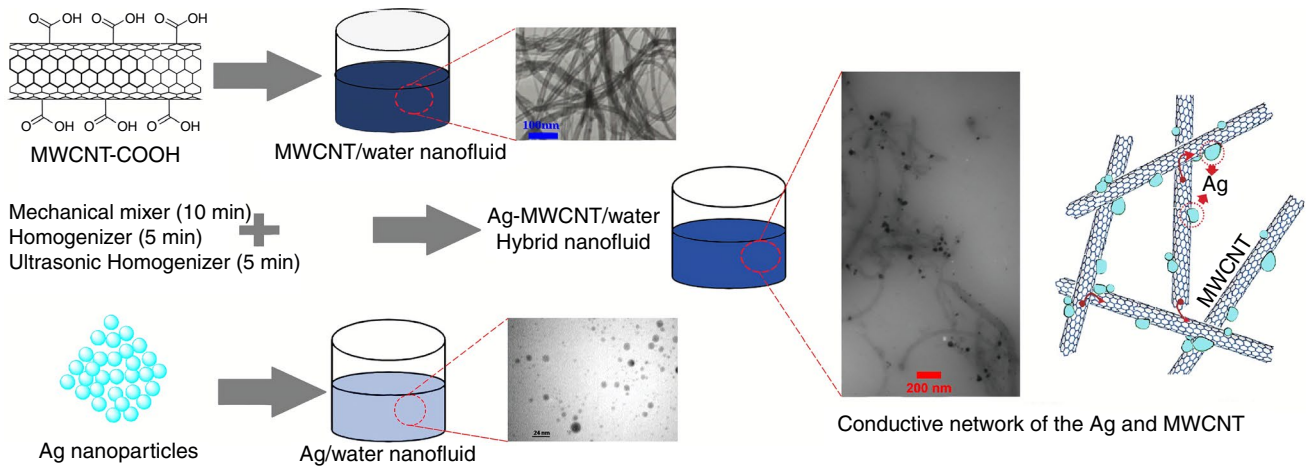

Fig. 1 Illustration of AgNPs@MWCNTs-COOH water-based nanofluid

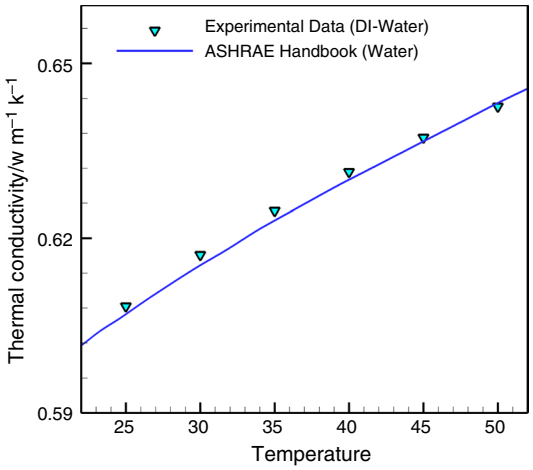

Fig. 2 Comparison between experimental and ASHRAE handbook data for DI water at different temperatures

Results and discussion

Material characterization

SEM and TEM evaluation

Morphological investigation of the prepared nanohybrid material was carried out to evaluate the successful procurement of modified MWCNTs-COOH with Ag nanoparticles (AgNPs@MWCNTs-COOH). For the aim, scanning-EM images of each nanomaterials were evaluated carefully. According to the SEM image of MWCNTs-COOH (Fig. 3a), a spaghetti-like porous reticular structure of multi-walled carbon nanotubes could be detected. Figure 3b illustrates the SEM image of modified MWCNTs with Ag nanoparticles. As it is obvious in this figure, the silver nanoparticles in nanometer size have been well distributed on the surface of MWCNTs-COOH. The mentioned observations from SEM image of AgNPs@MWCNTs-COOH can prove the successful decoration of multi-walled carbon nanotubes-COOH

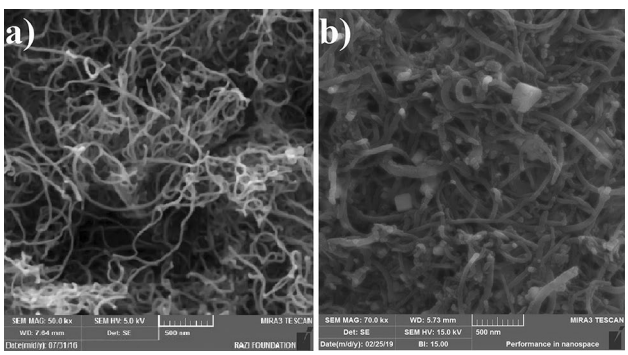

Fig. 3 SEM images of MWCNTs-COOH (**a**) and AgNPs@MWCNTs-COOH (**b**)

with Ag nanoparticles. TEM technique was used for further morphological investigation of the prepared nanocomposite. Figure 4a, b illustrates the TEM image of multi-walled carbon nanotubes-COOH and Ag nanoparticles, respectively. Figure 4c shows the TME image of AgNPs@MWCNTs-COOH. As it is illustrated in this figure (Fig. 4c), the surface of MWCNTs-COOH is appropriately modified with spherical-shaped silver nanoparticles.

XPS investigation

The X-ray photoelectron spectroscopy data of decorated MWCNTs-COOH with silver NPs are demonstrated in Fig. 5a. As it is demonstrated in Fig. 5b, the observed peaks at 284.8 and 286.4 eV are assigned to C–C (carbon) of graphite and C–O, respectively. The observed additional peak at 288.9 eV is related to the C atom in COOH functional groups on the surface of MWCNTs. The presence of COOH groups on the surface of multi-walled carbon nanotubes made the material more hydrophilic, and therefore, the material has more appropriate sites for coupling with Ag nanoparticles. The observed peaks at 368.11 eV and 374.13 eV are related to the 3d5/2 and 3d3/2 of silver, respectively. The obtained 3d doublet spin-orbit splitting of silver is approximately 6 eV, and the observation can prove that silver is in the zero valence state (Ag^0) and it is in the metallic form. In the spectrum of the material, there is not observed any peaks for 3d of silver in oxide states, and the observation can prove that silver nanoparticles are stable in the atmosphere. The peak at 532.7 is related to the surface oxygen atoms of multi-walled carbon nanotubes-COOH.

Thermal conductivity study

Figure 6 indicates the thermal conductivity of the resulting hybrid nanofluids with varying concentrations as a function of different temperatures. As shown by the results, the thermal conductivity of the hybrid nanofluid is dependent on the measured temperature and the MWCNTs/Ag material concentration. The hybrid nanofluid with a higher concentration of MWCNTs/Ag material for each measured temperature from 20 to 60 °C has higher thermal conductivity, and increasing the temperature raises the thermal conductivity for each hybrid nanofluid. It is possible to attribute an increase in thermal conductivity, based on temperature, to an increase in improvement of nanofluid molecules level in higher temperature and kinetic energy of them. Such increase shows the essential role that the temperature plays in improvement of the nanofluid's thermal conductivity. As the stability of fluid layer around the nanoparticle is greater than the overall fluid, the former shows higher thermal conductivity. Integration of this layer around the particle is such that it can be regarded as a part of nanoparticle. As the

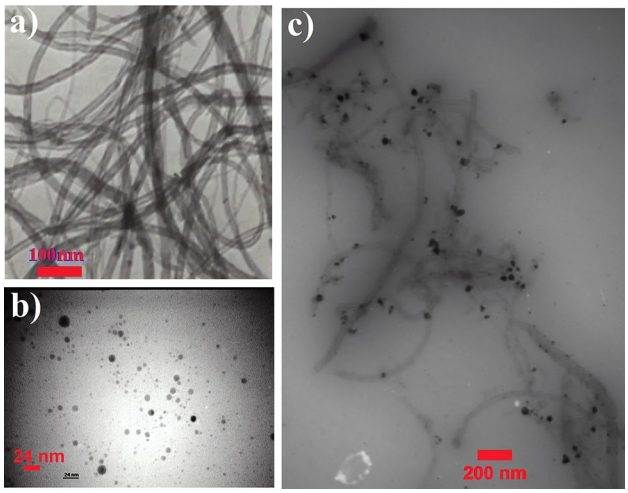

Fig. 4 TEM images of MWCNTs-COOH (**a**), AgNPs (**b**) and AgNPs@MWCNTs-COOH (**c**)

temperature increases, movement of nanoparticle movement is increased. As the collisions between surface atom fluid molecules and nanofluid are greater, thermal conductivity is increased. Because of an increase in the temperature, thermal conductivity increases, and volume fractions can be assigned to detachment of intermolecular bonds available in the fluid layers, increased Brownian motion, and increased collisions between nanoparticles. When aggregation and volume fraction of nanoparticles are increased, clusters of nanoparticle are formed. The formation of clusters provides the chance for faster heat transfer from these solid regions compared to liquids leading to more thermal conductivity. A simultaneous rise in volume fraction and temperature, the impacts of particle clustering and Brownian motion lead to a considerable increase in thermal conductivity. As increasing temperature increases Brownian motion, increased volume fraction at higher temperatures has a more impact on increasing thermal conductivity. When the volume fraction is low, the temperature has a lower impact on the thermal conductivity. When the volume fraction is increased, the impact of an increase in temperature is intensified because the increase in random motion amplifies the Brownian motion impact [58, 59]. The thermal conductivity shows a nonlinear increase with volume fraction and with temperature, and it shows consistency with another literature works [60, 61]. Figure 7 indicates the amount of relative thermal conductivity of nanofluid in comparison with the base fluid. The hybrid nanofluid's thermal conductivity was enhanced at varying temperatures and solid volume fraction about 19–47%. The

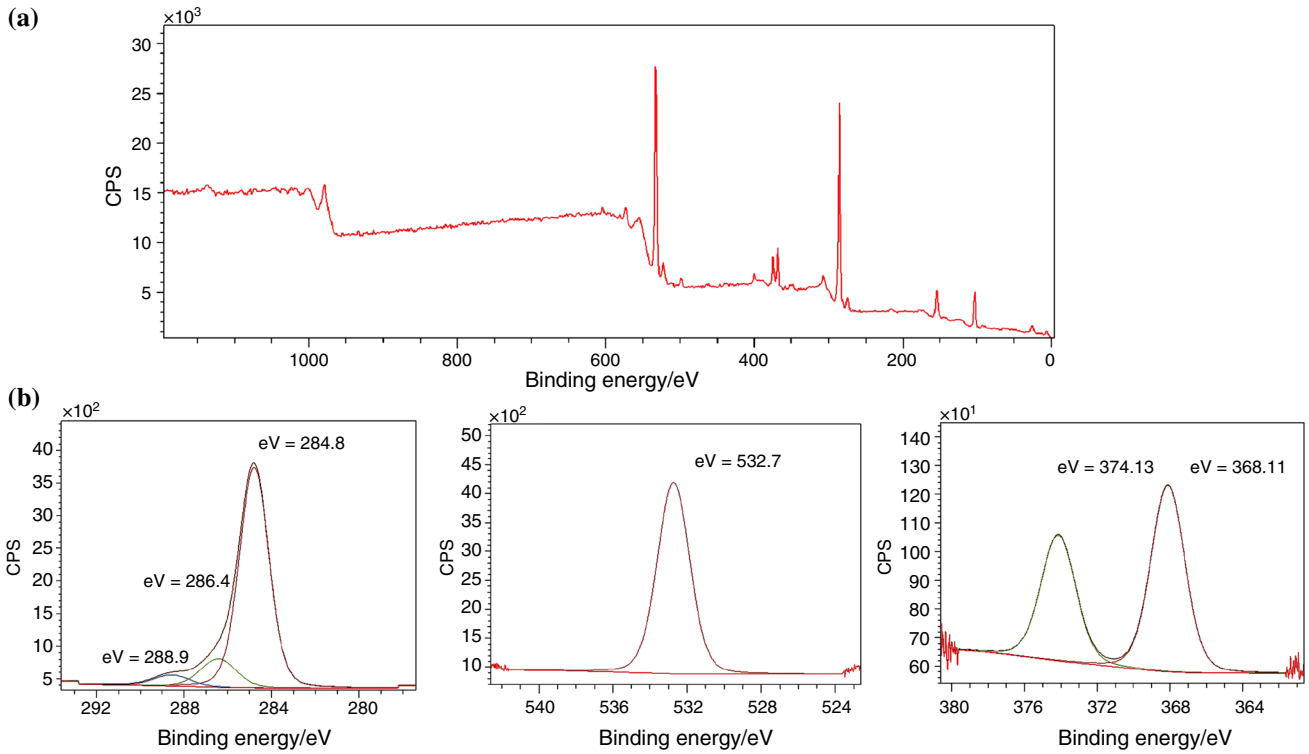

Fig. 5 XPS spectra of AgNPs@MWCNTs-COOH (**a**); and high-resolution of C1*s*, O1*s* and Ag3*d* spectrum for prepared nanocomposite (**b**)

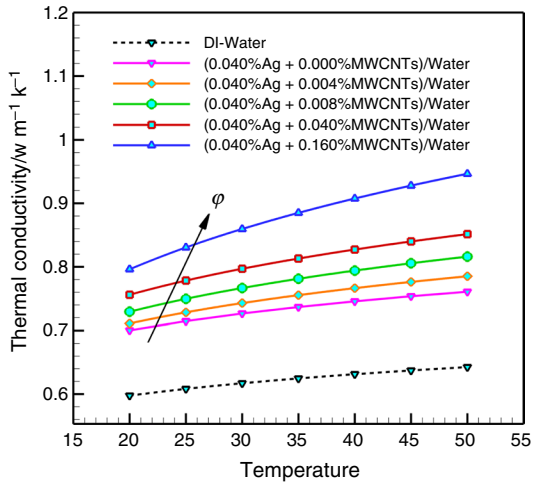

Fig. 6 Effects of φ on the thermal conductivity for different temperatures

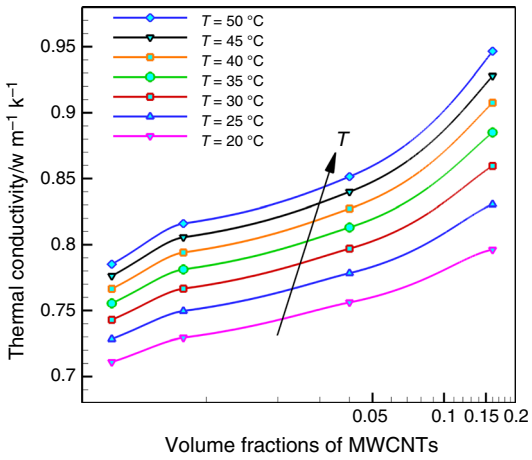

Fig. 8 Effects of T on the thermal conductivity for different solid volume fraction

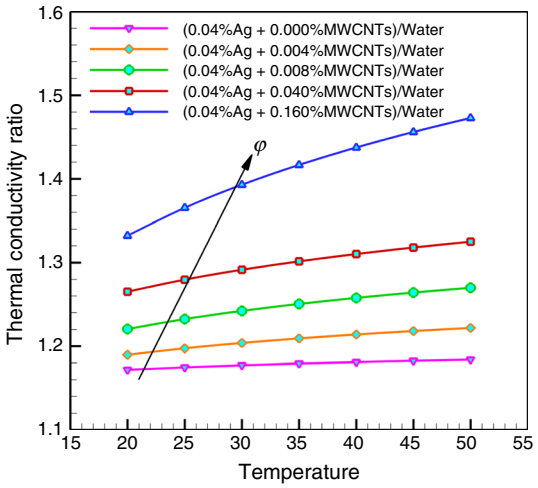

Fig. 7 Effects of φ on the thermal conductivity ratio for different temperatures

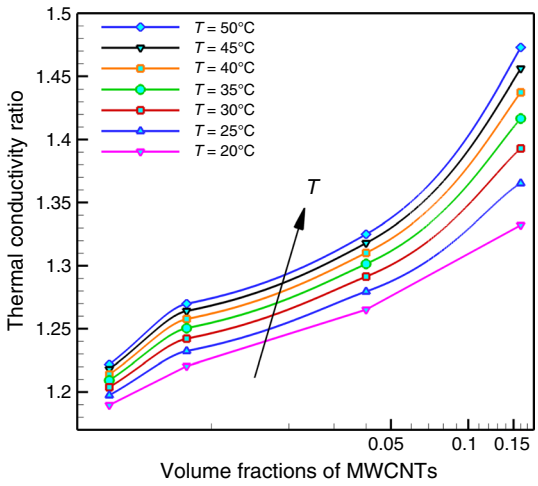

Fig. 9 Effects of T on the thermal conductivity ratio for different solid volume fraction

highest enhancement of hybrid nanofluids' thermal conductivity was observed at 50 °C. The hybrid nanofluids' thermal conductivity based on a volume fraction at the experimental temperature is indicated in Fig. 8. As observed in data, increasing volume fraction and temperature increased thermal conductivity. Figure 9 indicates the measured improved thermal conductivity ratio of COOH-functionalized MWCNTs/Ag–water hybrid nanofluid as a function of the solid volume fraction in varying temperatures. Increasing the volume fraction has a larger impact when the two variables (solid volume fraction and temperatures) are compared. As the volume fraction is decreased, the impact of temperature reduces. Moreover, when the volume fraction is increased, the impact of a temperature increase on thermal conductivity of hybrid nanofluid is augmented because the Brownian motion impact amplifies with increasing temperature. It is because of higher occurrence of random motion. As the temperature rises, movement of nanoparticle increases. Thus, because of higher occurrence of collisions between fluid molecules and surface atoms, thermal conductivity is improved [62]. Furthermore, the temperature does not have a significant impact at a low concentration of hybrid nanofluid, while its impact is greater at higher concentrations. For clarification, consider a certain volume of the hybrid nanofluid: as the solid volume fraction is increased, the amount of collisions is increased because of Brownian motion of particles. On the other hand, as the temperature is increased, the MWCNTs kinetic energy increases in the hybrid nanofluid.

Table 3 Enhancement of thermal conductivity of hybrid nanofluid at different concentrations and temperatures

Concentration/vol%	$T=20$ °C/%	$T=25$°C/%	$T=30$°C/%	$T=35$°C/%	$T=40$°C/%	$T=45$°C/%	$T=50$ °C/%
Ag:0.04% + MWCNTs-COOH:0.004%	18.96	19.74	20.38	20.92	21.39	21.80	22.17
Ag:0.04% + MWCNTs-COOH:0.008%	22.04	23.23	24.21	25.04	25.77	26.41	26.98
Ag:0.04% + MWCNTs-COOH:0.040%	26.51	27.95	29.14	30.14	31.02	31.80	32.50
Ag:0.04% + MWCNTs-COOH:0.160%	33.21	36.53	39.29	41.66	43.75	45.61	47.29

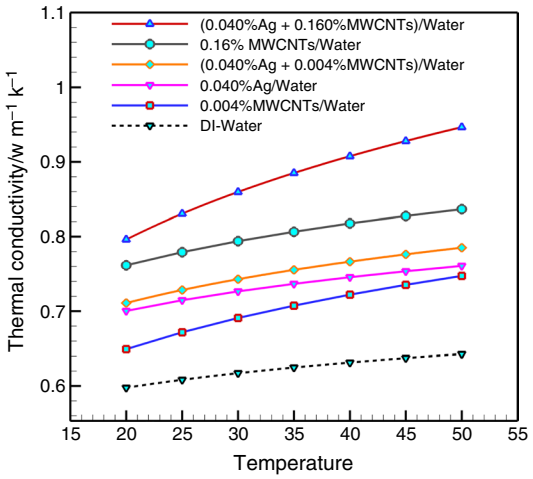

Fig. 10 Comparison of thermal conductivity for various mono and hybrid nanofluid

Thus, the number of collisions among the nanoparticles is raised. Hence, impacts of increasing the solid volume fraction are boosted by increasing the temperature [50]. Table 3 also shows enhancement of thermal conductivity of hybrid nanofluid at different concentrations and temperature. The synergistically improved impact of thermal conductivity of water-based MWCNTs/Ag hybrid nanofluid between Ag/water and MWCNTs/water nanofluids is represented in Fig. 10. This figure confirms high efficiency of our material for improving the thermal conductivity of nanofluid in comparison with MWCNTs nanofluid or Ag nanoparticles. It is because of the synergistic impact of high thermally conducting individual components like Ag nanoparticles and MWCNTs. In addition, if MWCNTs and Ag nanoparticles are added, the overall surface area is increased in the hybrid nanofluid. Therefore, the thermal conductivity of the hybrid nanofluids is improved. Hence, the hybrid materials have synergistic characteristics in compression with the single nanoparticles. Also, Table 4 shows that comparison of enhancement thermal conductivity data for water-based COOH-MWCNTs/Ag hybrid nanofluid with Ag/water and MWCNTs-COOH/water nanofluid.

Proposing new correlation for calculation of the thermal conductivity ratio

Various theoretical approaches can be used for evaluating the thermal conductivity of nanofluids for anticipating and comparing with the empirical findings. The classical models like Hamilton–Crosser and Maxwell are popular for anticipating the thermal conductivity of well-dispersed fluids having solid particles. For highly limited works of authors in the hybrid nanofluids field, a few numbers of limited models have been proposed up to now for estimation of thermophysical characteristics of these nanofluids. On the other hand, many of the classical models do not address the hybrid nanofluids, and their feature alterations are not accurately estimated because these models do not consider the impact of the thermal interface resistance between the base fluid and hybrid material, and they are just used for spherical particles [63]. Thus, a simple correlation with the proper precision is also suggested in the current work for predicting the results of the hybrid nanofluids thermal conductivity ratio.

Table 4 Comparison of enhancement thermal conductivity data for water-based MWCNTs-COOH/Ag hybrid nanofluid with Ag/water and MWCNTs-COOH/water nanofluid

Concentration /vol%	$T=20$°C/%	$T=25$°C/%	$T=30$°C/%	$T=35$°C/%	$T=40$°C/%	$T=45$°C/%	$T=50$°C/%
MWCNTs-COOH:0.004%	8.58	10.41	11.93	13.23	14.37	15.38	16.30
Ag:0.04%	17.18	17.48	17.72	17.92	18.10	18.25	18.39
Ag:0.04% + MWCNTs-COOH:0.004%	18.96	19.74	20.38	20.92	21.39	21.80	22.17
MWCNTs-COOH:0.160%	27.43	28.09	28.64	29.10	29.50	29.85	30.17
Ag:0.04% + MWCNTs-COOH:0.16%	33.21	36.53	39.29	41.66	43.75	45.61	47.29

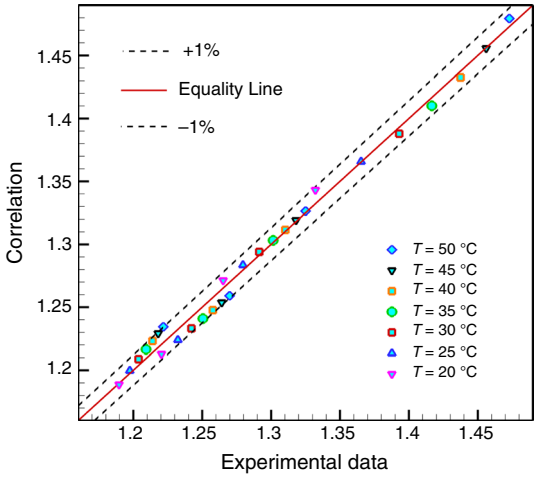

Fig. 11 Comparisons between experimental data and formula outputs for thermal conductivity

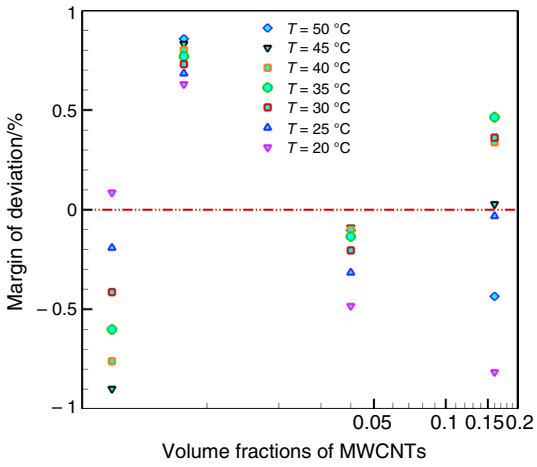

Fig. 12 Calculated margin of deviation for all data

As shown by the empirical data on the thermal conductivity of COOH-functionalized MWCNTs/Ag–water hybrid nanofluid with changes in the nanocomposite temperature and concentrations (two significant factors that influence on thermal conductivity ratio [64, 65]), a new correlation was conducted for calculating thermal conductivity ratio using curve fitting approach based on Marquardt–Levenberg algorithm [66]. It provides a high accuracy with $R^2 = 0.992$. This correlation uses the rule of the mixture model [67] with the equation as follows:

$$\frac{k_{\mathrm{hnf}}}{k_{\mathrm{bf}}} = aT^{\mathrm{b}} + c\varphi^{\mathrm{d}} + e(T\varphi)^{\mathrm{f}} - g \tag{3}$$

In this correlation, φ denotes the nanocomposite concentration, T denotes the temperature, and $k_{\mathrm{hnf}}/k_{\mathrm{bf}}$ denotes the thermal conductivity ratio. Additionally, the hnf and bf subscripts represent hybrid nanofluid and base fluid, respectively. In this equation, the constant values are:

$$\begin{aligned} &a = 125/44366318;\ b = 0/00039598240056; c = 342/1123212\\ &d = 0/00010161334154; e = 0/0039849271853\\ &f = 1/6256254647; g = 466/32447742 \end{aligned} \tag{4}$$

Figure 11 indicates the comparison between the values taken from proposed formula and the empirical data with an absolute average deviation of 0.59% and standard deviation of 0.81%. The two dashed lines shown in this figure are the 99% prediction bounds. This comparison is used for the solid concentrations and all temperatures. It is observed that the correlation has presented adequate results, and it can be used for engineering applications with a coefficient of determination (R^2) of 0.992.

Moreover, a parameter known as marginal deviation is developed for verifying the suggested correlation accuracy, which is given as:

$$\text{Deviation margin} = \left[\frac{\left(\frac{k_{\mathrm{hnf}}}{k_{\mathrm{bf}}}\right)_{\mathrm{exp}} - \left(\frac{k_{\mathrm{hnf}}}{k_{\mathrm{bf}}}\right)_{\mathrm{corr}}}{\left(\frac{k_{\mathrm{hnf}}}{k_{\mathrm{bf}}}\right)_{\mathrm{corr}}}\right] \times 100 \tag{5}$$

where exp and corr subscripts denote the empirical results and the results predicted by the proposed formula, respectively. The accuracy of the proposing formula between experimental values and predicted data is also evaluated in Fig. 12. As seen, most points have the deviation less than 1%, which is appropriate for an empirical correlation. Figure 13 displays the more accurate comparison of the experimental data with the proposed formula as a function of hybrid nanofluid concentration at varying temperatures. As their advantages, these figures show the difference between the experimental results and model outputs in each experiment.

Uncertainty calculation

The uncertainty of the obtained data was calculated from the bias error (equipment) and precision error obtained from the deviation in the experimental results. The bias error in monitoring of thermal conductivity by KD2 Pro was ± 5%. The bias error for the weighing scale (Adventurer, Ohaus, Nanikon, Switzerland) and temperature (Pt100 sensors Class A) was ± 0.001 g and ± 0.1 °C. The uncertainty of the experiment is obtained by the following [68–70]:

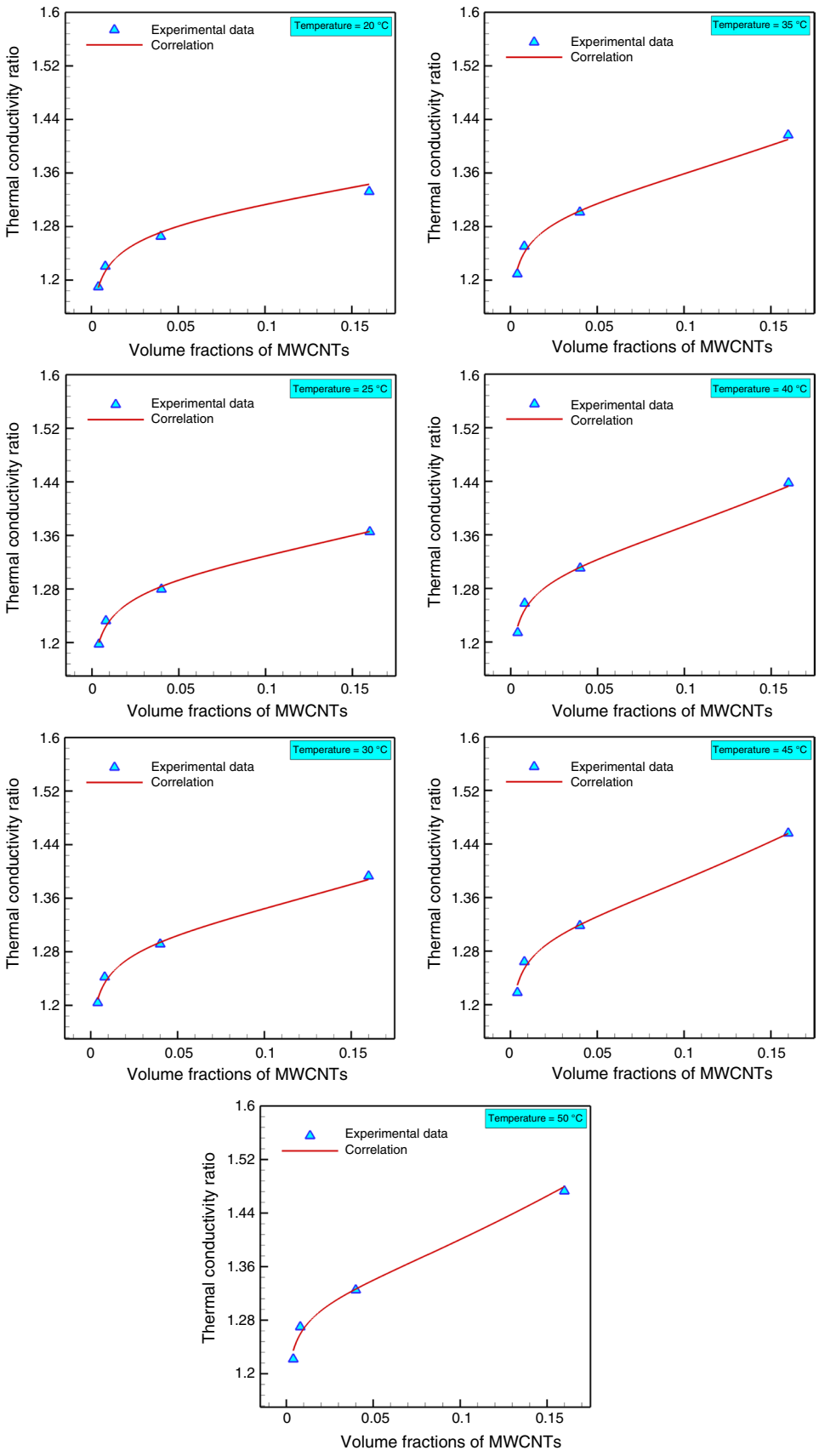

Fig. 13 Curve fitting on experiment results based on proposed formula at different temperatures

$$u = \pm\sqrt{u_b^2 + u_p^2} \tag{6}$$

$$u_b = \pm\sqrt{\left(\frac{\Delta k}{k}\right)^2 + \left(\frac{\Delta w}{w}\right)^2 + \left(\frac{\Delta T}{T}\right)^2} \tag{7}$$

$$u_p = \pm\, t_{v,p}\mathrm{SD} \tag{8}$$

where U_B, U_p, $t_{v,p}$ and SD are bias error, precision or random error in measurement with $p\%$ probability, weighing function for v degree of freedom and $p\%$ probability (95%) and sample standard deviation, respectively. According to the presented definitions, the obtained uncertainty percent for the obtained data was between 6.44% and 8.95%.

Conclusions

In conclusion, Ag-decorated MWCNTs/water hybrid nanofluid was successfully prepared via two-step method. Improvement of thermal conductivity of the hybrid nanofluid shows a synergistic impact between MWCNTs and Ag nanoparticles based on following factors: (1) highly thermal conductive MWCNTs receive and transport heat from the Ag, facilitating further heat dissipation; (2) an adequate two-dimensional well-interconnected MWCNTs/Ag nanostructure establishing more efficient heat transfer networks; (3) Ag nanoparticles and MWCNTs increase the overall surface area in the hybrid nanofluid. The diagrammatic depiction for synergistic impact on heat conductive network established by MWCNTs and Ag nanoparticles is also proposed. Using experimental data, the thermal conductivity ratio showed that the highest improvement of thermal conductivity of hybrid nanofluid was 47.3%. This was observed at 50 °C for hybrid nanofluid having 0.04 vol% Ag nanoparticles and 0.16 vol% MWCNT-COOH materials. According to the analysis, it is found that nanocomposite-based hybrid nanofluids (MWCNTs/Ag) have better the thermal characteristics compared to the single-nanoparticle-based nanofluids (MWCNTs or Ag). Therefore, these hybrid nanofluids serve as the future nanofluids for heat exchange devices. As the last point, a new correlation was suggested using empirical data for anticipating the thermal conductivity ratio of MWCNTs-COOH/Ag/water hybrid nanofluid. The highest value of deviation margin was 1%. According to the comparisons, there was a very good consistency between the empirical data and correlation outputs.

References

1. Moya M, Bruno JC, Eguia P, Torres E, Zamora I, Coronas A. Performance analysis of a trigeneration system based on a micro gas turbine and an air-cooled, indirect fired, ammonia-water absorption chiller. Appl Energy. 2011;88:4424–40.
2. Calise F. Design of a hybrid polygeneration system with solar collectors and a solid oxide fuel cell: dynamic simulation and economic assessment. Int J Hydrogen Energy. 2011;36:6128–50.
3. Choi SUS. Enhancing thermal conductivity of fluids with nanoparticles. In: Proceedings of the ASME international mechanical engineering congress and exposition. San Francisco: ASME, FED; 1995. p. 99–105.
4. Patel HE, Das SK, Sundararajan T, Sreekumaran Nair A, George B, Pradeep T. Thermal conductivities of naked and monolayer protected metal nanoparticle based nanofluids: manifestation of anomalous enhancement and chemical effects. Appl Phys Lett. 2003;83:2931–3.
5. Khoshvaght-Aliabadi M, Hormozi F. Investigation on heat transfer and pressure drop of copper-water nanofluid flow in plain and perforated channels. Exp Heat Transf. 2016;29:427–44.
6. Noghrehabadi A, Pourrajab R. Experimental investigation of forced convective heat transfer enhancement of γ-Al_2O_3/water nanofluid in a tube. J Mech Sci Technol. 2016;30:943–52.
7. Noghrehabadi A, Pourrajab R, Ghalambaz M. Effect of partial slip boundary condition on the flow and heat transfer of nanofluids past stretching sheet prescribed constant wall temperature. Int J Therm Sci. 2012;54:253–61.
8. Noghrehabadi A, Pourrajab R, Ghalambaz M. Flow and heat transfer of nanofluids over stretching sheet taking into account partial slip and thermal convective boundary conditions. Heat Mass Transf und Stoffuebertragung. 2013;49:1357–66.
9. Moreira LM, Carvalho EA, Bell MJV, Anjos V, Sant' Ana AC, Alves APP, et al. Thermo-optical properties of silver and gold nanofluids. J Therm Anal Calorim. 2013;114:557–64.
10. Sheikholeslami M. Numerical approach for MHD Al_2O_3-water nanofluid transportation inside a permeable medium using innovative computer method. Comput Methods Appl Mech Eng. 2019;344:306–18.
11. Fadodun OG, Amosun AA, Okoli NL, Olaloye DO, Durodola SS, Ogundeji JA. Sensitivity analysis of entropy production in Al_2O_3/H_2O nanofluid through converging pipe. J Therm Anal Calorim. 2019. https://doi.org/10.1007/s10973-019-09163-y.
12. Sheikholeslami M. New computational approach for exergy and entropy analysis of nanofluid under the impact of Lorentz force through a porous media. Comput Methods Appl Mech Eng. 2019;344:319–33.
13. Shahsavar A, Godini A, Sardari PT, Toghraie D, Salehipour H. Impact of variable fluid properties on forced convection of Fe_3O_4/CNT/water hybrid nanofluid in a double-pipe mini-channel heat exchanger. J Therm Anal Calorim. 2019;137:1031–43.
14. Sheikholeslami M. Magnetic field influence on CuO–H_2O nanofluid convective flow in a permeable cavity considering various shapes for nanoparticles. Int J Hydrogen Energy. 2017;42:19611–21.
15. Sheikholeslami M, Jafaryar M, Shafee A, Li Z. Nanofluid heat transfer and entropy generation through a heat exchanger considering a new turbulator and CuO nanoparticles. J Therm Anal Calorim. 2018;134:2295–303.
16. Bahiraei M, Hangi M, Saeedan M. A novel application for energy efficiency improvement using nanofluid in shell and tube heat exchanger equipped with helical baffles. Energy. 2015;93:2229–40.

17. Ali HM, Ali H, Liaquat H, Bin Maqsood HT, Nadir MA. Experimental investigation of convective heat transfer augmentation for car radiator using ZnO-water nanofluids. Energy. 2015;84:317–24.
18. Seyednezhad M, Sheikholeslami M, Ali JA, Shafee A, Nguyen TK. Nanoparticles for water desalination in solar heat exchanger. J Therm Anal Calorim. 2019. https://doi.org/10.1007/s10973-019-08634-6.
19. Kasaeian A, Eshghi AT, Sameti M. A review on the applications of nanofluids in solar energy systems. Renew Sustain Energy Rev. 2015;43:584–98.
20. Jouybari HJ, Nimvari ME, Saedodin S. Thermal performance evaluation of a nanofluid-based flat-plate solar collector: an experimental study and analytical modeling. J Therm Anal Calorim. 2019;137:1757–74.
21. Mohebbi R, Mehryan SAM, Izadi M, Mahian O. Natural convection of hybrid nanofluids inside a partitioned porous cavity for application in solar power plants. J Therm Anal Calorim. 2019;137:1719–33.
22. Zeng J, Xuan Y. Enhanced solar thermal conversion and thermal conduction of MWCNT-SiO_2/Ag binary nanofluids. Appl Energy. 2018;212:809–19.
23. Rajendran DR, Ganapathy Sundaram E, Jawahar P, Sivakumar V, Mahian O, Bellos E. Review on influencing parameters in the performance of concentrated solar power collector based on materials, heat transfer fluids and design. J Therm Anal Calorim. 2019. https://doi.org/10.1007/s10973-019-08759-8.
24. Xie H, Chen L. Review on the preparation and thermal performances of carbon nanotube contained nanofluids. J Chem Eng Data. 2011;56:1030–41.
25. Rasheed AK, Khalid M, Rashmi W, Gupta TCSM, Chan A. Graphene based nanofluids and nanolubricants—review of recent developments. Renew Sustain Energy Rev. 2016;63:346–62.
26. Van Trinh P, Anh NN, Thang BH, Quang LD, Hong NT, Hong NM, et al. Enhanced thermal conductivity of nanofluid-based ethylene glycol containing Cu nanoparticles decorated on a Gr-MWCNT hybrid material. RSC Adv. Royal Society of Chemistry. 2017;7:318–26.
27. Sparavigna A. Lattice specific heat of carbon nanotubes. J Therm Anal Calorim. 2008;93:983–6.
28. Sarkar J, Ghosh P, Adil A. A review on hybrid nanofluids: recent research, development and applications. Renew Sustain Energy Rev. 2015;43:164–77.
29. Ghalambaz M, Doostani A, Izadpanahi E, Chamkha AJ. Conjugate natural convection flow of Ag–MgO/water hybrid nanofluid in a square cavity. J Therm Anal Calorim. 2019. https://doi.org/10.1007/s10973-019-08617-7.
30. Ghalambaz M, Mehryan SAM, Izadpanahi E, Chamkha AJ, Wen D. MHD natural convection of Cu–Al_2O_3 water hybrid nanofluids in a cavity equally divided into two parts by a vertical flexible partition membrane. J Therm Anal Calorim. 2019;138:1723–43.
31. Pourrajab R, Noghrehabadi A, Hajidavalloo E, Behbahani M. Investigation of thermal conductivity of a new hybrid nanofluids based on mesoporous silica modified with copper nanoparticles: synthesis, characterization and experimental study. J Mol Liq. 2019. https://doi.org/10.1016/j.molliq.2019.112337.
32. Esfe MH, Rejvani M, Karimpour R, Abbasian Arani AA. Estimation of thermal conductivity of ethylene glycol-based nanofluid with hybrid suspensions of SWCNT–Al_2O_3 nanoparticles by correlation and ANN methods using experimental data. J Therm Anal Calorim. 2017;128:1359–71.
33. Abbasi S, Zebarjad SM, Baghban SHN, Youssefi A, Ekrami-Kakhki MS. Experimental investigation of the rheological behavior and viscosity of decorated multi-walled carbon nanotubes with TiO_2 nanoparticles/water nanofluids. J Therm Anal Calorim. 2016;123:81–9.
34. Shanbedi M, Zeinali Heris S, Maskooki A. Experimental investigation of stability and thermophysical properties of carbon nanotubes suspension in the presence of different surfactants. J Therm Anal Calorim. 2015;120:1193–201.
35. Ranjbar S, Masoumi H, Haghighi Khoshkhoo R, Mirfendereski M. Experimental investigation of stability and thermal conductivity of phase change materials containing pristine and functionalized multi-walled carbon nanotubes. J Therm Anal Calorim. 2019;137:1723–43.
36. Turcu R, Darabont A, Nan A, Aldea N, Macovei D, Bica D, et al. New polypyrrole-multiwall carbon nanotubes hybrid materials. J Optoelectron Adv Mater. 2006;8:643–7.
37. Jha N, Ramaprabhu S. Thermal conductivity studies of metal dispersed multiwalled carbon nanotubes in water and ethylene glycol based nanofluids. J Appl Phys. 2009;106:084317.
38. Rostamian SH, Biglari M, Saedodin S, Hemmat Esfe M. An inspection of thermal conductivity of CuO-SWCNTs hybrid nanofluid versus temperature and concentration using experimental data, ANN modeling and new correlation. J Mol Liq. 2017;231:364–9.
39. Megatif L, Ghozatloo A, Arimi A, Shariati-Niasar M. Investigation of laminar convective heat transfer of a novel TiO_2-Carbon nanotube hybrid water-based nanofluid. Exp Heat Transf. 2016;29:124–38.
40. Nine MJ, Batmunkh M, Kim JH, Chung HS, Jeong HM. Investigation of Al_2O_3-MWCNTs hybrid dispersion in water and their thermal characterization. J Nanosci Nanotechnol. 2012;12:4553–9.
41. Shahsavar A, Salimpour MR, Saghafian M, Shafii MB. An experimental study on the effect of ultrasonication on thermal conductivity of ferrofluid loaded with carbon nanotubes. Thermochim Acta. 2015;617:102–10.
42. Chen LF, Cheng M, Yang DJ, Yang L. Enhanced thermal conductivity of nanofluid by synergistic effect of multi-walled carbon nanotubes and Fe_2O_3 nanoparticles. Appl Mech Mater. 2014;548–549:118–23.
43. Zadkhast M, Toghraie D, Karimipour A. Developing a new correlation to estimate the thermal conductivity of MWCNT-CuO/water hybrid nanofluid via an experimental investigation. J Therm Anal Calorim. 2017;129:859–67.
44. Farbod M, Ahangarpour A. Improved thermal conductivity of Ag decorated carbon nanotubes water based nanofluids. Phys Lett Sect A Gen At Solid State Phys. 2016;380:4044–8.
45. Munkhbayar B, Tanshen MR, Jeoun J, Chung H, Jeong H. Surfactant-free dispersion of silver nanoparticles into MWCNT-aqueous nanofluids prepared by one-step technique and their thermal characteristics. Ceram Int. 2013;39:6415–25.
46. Lee G-W, Lee JI, Sang-Soo L, Park M, Kim J. Comparisons of thermal properties between inorganic filler and acid-treated multiwall nanotube/polymer composites. J Mater Sci. 2005;40:1259–63.
47. Ghose S, Watson KA, Working DC, Connell JW, Smith JG Jr, Sun YP. Thermal conductivity of ethylene vinyl acetate copolymer/nanofiller blends. Compos Sci Technol. 2008;68:1843–53.
48. Munkhbayar B, Hwang S, Kim J, Bae K, Ji M, Chung H, et al. Photovoltaic performance of dye-sensitized solar cells with various MWCNT counter electrode structures produced by different coating methods. Electrochim Acta. 2012;80:100–7.
49. Munkhbayar B, Nine MJ, Hwang S, Kim J, Bae K, Chung H, et al. Effect of grinding speed changes on dispersibility of the treated multi-walled carbon nanotubes in aqueous solution and

its thermal characteristics. Chem Eng Process Process Intensif. 2012;61:36–41.
50. Hemmat Esfe M, Saedodin S, Mahian O, Wongwises S. Thermophysical properties, heat transfer and pressure drop of COOH-functionalized multi walled carbon nanotubes/water nanofluids. Int Commun Heat Mass Transf. 2014;58:176–83.
51. Dalkılıç AS, Türk OA, Mercan H, Nakkaew S, Wongwises S. An experimental investigation on heat transfer characteristics of graphite-SiO_2/water hybrid nanofluid flow in horizontal tube with various quad-channel twisted tape inserts. Int Commun Heat Mass Transf. 2019;107:1–13.
52. Sedeh RN, Abdollahi A, Karimipour A. Experimental investigation toward obtaining nanoparticles' surficial interaction with basefluid components based on measuring thermal conductivity of nanofluids. Int Commun Heat Mass Transf. 2019;103:72–82.
53. Sarafraz MM, Yang B, Pourmehran O, Arjomandi M, Ghomashchi R. Fluid and heat transfer characteristics of aqueous graphene nanoplatelet (GNP) nanofluid in a microchannel. Int Commun Heat Mass Transf. 2019;107:24–33.
54. Ghaffarkhah A, Bazzi A, Azimi Dijvejin Z, Talebkeikhah M, Keshavarz Moraveji M, Agin F. Experimental and numerical analysis of rheological characterization of hybrid nano-lubricants containing COOH-Functionalized MWCNTs and oxide nanoparticles. Int Commun Heat Mass Transf. 2019;101:103–15.
55. Nagasaka Y, Nagashima A. Absolute measurement of the thermal conductivity of electrically conducting liquids by the transient hot-wire method. J Phys E. 1981;14:1435–40.
56. Yamasue E, Susa M, Fukuyama H, Nagata K. Thermal conductivities of silicon and germanium in solid and liquid states measured by non-stationary hot wire method with silica coated probe. J Cryst Growth. 2002;234:121–31.
57. Howell RH. Principles of heating ventilating and air conditioning: a textbook with design data based on the 2017 Ashrae handbook fundamentals. ASHRAE; 2017.
58. Li FC, Yang JC, Zhou WW, He YR, Huang YM, Jiang BC. Experimental study on the characteristics of thermal conductivity and shear viscosity of viscoelastic-fluid-based nanofluids containing multiwalled carbon nanotubes. Thermochim Acta. 2013;556:47–53.
59. Chon CH, Kihm KD, Lee SP, Choi SUS. Empirical correlation finding the role of temperature and particle size for nanofluid (Al_2O_3) thermal conductivity enhancement. Appl Phys Lett. 2005;87:1–3.
60. Baby TT, Sundara R. Synthesis and transport properties of metal oxide decorated graphene dispersed nanofluids. J Phys Chem C. 2011;115:8527–33.
61. Das SK, Choi SUS, Patel HE. Heat transfer in nanofluids—a review. Heat Transf Eng. 2006;27:3–19.
62. Esfahani NN, Toghraie D, Afrand M. A new correlation for predicting the thermal conductivity of ZnO–Ag (50%–50%)/water hybrid nanofluid: an experimental study. Powder Technol. 2018;323:367–73.
63. Mohamed RA, Habashy DM. Thermal conductivity modeling of propylene glycol-based nanofluid using artificial neural network. J Adv Phys. 2018;14:5281–91.
64. Mousavi SM, Esmaeilzadeh F, Wang XP. Effects of temperature and particles volume concentration on the thermophysical properties and the rheological behavior of CuO/MgO/TiO_2 aqueous ternary hybrid nanofluid: experimental investigation. J Therm Anal Calorim. 2019;137:879–901.
65. Hemmat-Esfe M, Esfandeh S, Rejvani M. Modeling of thermal conductivity of MWCNT-SiO_2 (30:70%)/EG hybrid nanofluid, sensitivity analyzing and cost performance for industrial applications: an experimental based study. J Therm Anal Calorim. 2018;131:1437–47.
66. Marquardt DW. An algorithm for least-squares estimation of nonlinear parameters. J Soc Ind Appl Math. 1963;11:431–41.
67. Askeland DR. The science and engineering of materials. Ontario: Nelson Education; 1994.
68. Figliola RS, Beasley DE. Theory and design for mechanical measurements. 2nd ed. New York: Wiley; 1995.
69. Sharifpur M, Tshimanga N, Meyer JP, Manca O. Experimental investigation and model development for thermal conductivity of α-Al_2O_3-glycerol nanofluids. Int Commun Heat Mass Transf. 2017;85:12–22.
70. Teng TP, Hung YH, Teng TC, Mo HE, Hsu HG. The effect of alumina/water nanofluid particle size on thermal conductivity. Appl Therm Eng. 2010;30:2213–8.